

Toward Guarantees for Clinical Reasoning in Vision Language Models via Formal Verification

Vikash Singh^{*1}, Debargha Ganguly^{*1}, Haotian Yu¹, Chengwei Zhou¹, Prerna Singh¹, Brandon Lee¹, Vipin Chaudhary¹, and Gourav Datta¹

Case Western Reserve University

vikash, debargha, haotian.yu, chengwei.zhou, prerna,
brandon.lee, vipin, gourav.datta@case.edu

Abstract. Vision-language models (VLMs) show promise in drafting radiology reports, yet they frequently suffer from logical inconsistencies, generating diagnostic impressions unsupported by their own perceptual findings or missing logically entailed conclusions. Standard lexical metrics heavily penalize clinical paraphrasing and fail to capture these deductive failures in reference-free settings. Toward guarantees for clinical reasoning, we introduce a neurosymbolic verification framework that deterministically audits the internal consistency of VLM-generated reports. Our pipeline autoformalizes free-text radiographic findings into structured propositional evidence, utilizing an SMT solver (Z3) and a clinical knowledge base to verify whether each diagnostic claim is mathematically entailed, hallucinated, or omitted. Evaluating seven VLMs across five chest X-ray benchmarks, our verifier exposes distinct reasoning failure modes, such as conservative observation and stochastic hallucination, that remain invisible to traditional metrics. On labeled datasets, enforcing solver-backed entailment acts as a rigorous post-hoc guarantee, systematically eliminating unsupported hallucinations to significantly increase diagnostic soundness and precision in generative clinical assistants.

Keywords: Vision Language Models · Neurosymbolic AI · Verification

1 Introduction

Unprecedented imaging volumes have accelerated the adoption of generative vision-language models (VLMs) as cognitive assistants in radiology [4, 17]. By drafting preliminary reports from visual context, models like MedGemma and LLaVA-Med aim to reduce clinician fatigue and turnaround times [23]. However, deploying these models in safety-critical clinical environments exposes a fundamental vulnerability: the absence of formal guarantees. In medicine, statistical plausibility is an insufficient proxy for correctness; practitioners must trust that generated drafts are deductively valid. Today, this trust is unfounded,

^{*} Equal contribution.

This work was supported in part by the NSF research grant #2112606, #2117439.

as VLMs function as probabilistic text generators optimized for fluency rather than verifiable clinical reasoning [2].

The core technical barrier to building verifiable VLMs lies in their autoregressive objective function [5]. A model generates a report by maximizing the likelihood of the next token, modeled as $P(w_t|w_{<t}, I)$. While this effectively captures correlations between visual features and clinical phrasing [20], it fundamentally precludes intrinsic mechanisms to guarantee logical entailment [16]. Consequently, a VLM may correctly perceive visual evidence in the “Findings” section (e.g., “blunted costophrenic angle”) yet fail to deduce the mathematically forced conclusion in the “Impression” (e.g., “pleural effusion”). Conversely, it may hallucinate unsupported diagnoses based on training priors [13]. This stochasticity creates a dangerous “illusion of reasoning” [24], entirely negating the technology’s assistive value when clinicians must expend effort debugging fluent but fundamentally contradictory logic [9].

Compounding this issue, current evaluation paradigms are entirely empirical and fail to capture deductive validity. Standard NLP metrics (BLEU [18], ROUGE [15]) and entity-aware scores (F1-CheXbert [22]) operate strictly on reference similarity against a ground-truth report. Unlike traditional software validation, which leverages formal methods to prove system properties, these metrics cannot assess the internal logical consistency of a generated report in isolation. In real-world clinical workflows where ground truth is intrinsically unavailable, these metrics offer no safety guarantees. A system that generates a fluent but self-contradictory report poses a severe risk of automation bias [19], underscoring the urgent need to transition from empirical string-matching to formal verification.

Toward providing formal guarantees for clinical reasoning, we propose a novel neurosymbolic verification framework that imposes formally verifiable constraints on the output of VLMs [11, 10]. Drawing on formal verification principles, we treat the internal logical consistency of a drafted radiology report as a formal satisfiability (SAT) problem [3]. Our pipeline explicitly decouples visual perception, handled probabilistically by the VLM, from clinical reasoning, which is audited deterministically by a symbolic solver [7, 21]. Our contributions are:

1. We introduce a reference-free neurosymbolic framework that bridges probabilistic text generation and deterministic logic. By mapping free-text findings into SMT constraints via a clinical ontology, we enable the automated, runtime verification of diagnostic logic *independently of ground-truth reference texts*.
2. Through the formal auditing of seven VLMs across five chest X-ray benchmarks, we expose distinct deductive failure modes, ranging from conservative observation to stochastic hallucination, that empirical, reference-based metrics are mathematically incapable of detecting.
3. We demonstrate that applying an SMT solver as a post-hoc deductive safeguard on labeled datasets provably eliminates unsupported hallucinations. This enforcement of mathematical entailment yields targeted, quantifiable

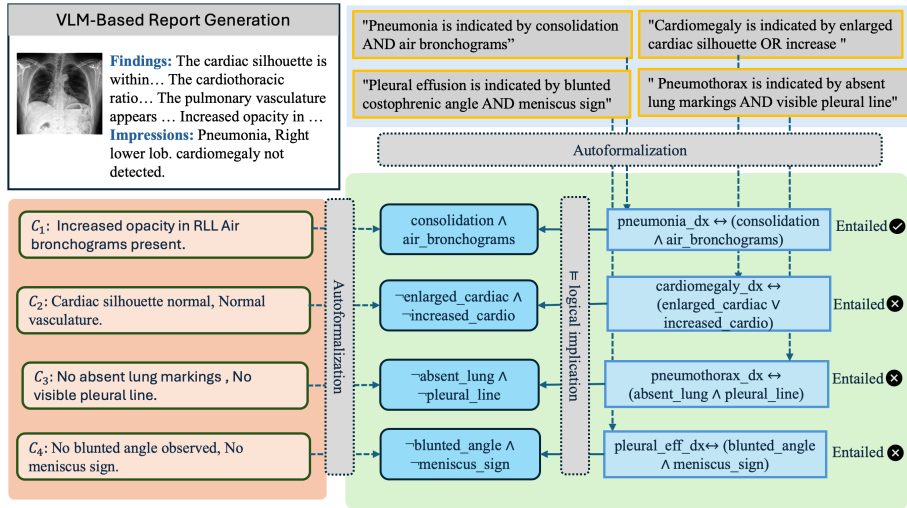


Fig. 1: Neurosymbolic verification pipeline. A VLM generates Findings and Impression text, which are autoformalized into structured evidence and checked against a clinical knowledge base using Z3 to verify clinical reasoning.

guarantees for diagnostic soundness and precision in generative clinical assistants.

2 Methodology

Given an image I and a VLM \mathcal{M}_θ , the model generates a report $R = (R_F, R_I)$ comprising a *Findings* section R_F and an *Impression* section R_I . Our objective is to verify whether the diagnostic claims in R_I are logically entailed by the perceptual evidence asserted in R_F under a fixed clinical knowledge base, effectively isolating visual perception from deductive reasoning to provide formal guarantees of internal consistency.

2.1 Ontological Grounding and Autoformalization

To transition from free text to a computable domain, we define a lightweight formal ontology $\mathcal{O} = \langle \mathcal{F}, \mathcal{D}, \mathcal{K} \rangle$. $\mathcal{F} = \{f_1, \dots, f_N\}$ is a finite set of atomic observational predicates (e.g., `costophrenic_blunting`), $\mathcal{D} = \{d_1, \dots, d_M\}$ is a set of diagnostic predicates (e.g., `pleural_effusion`), and \mathcal{K} represents the clinical knowledge base, modeled as a set of propositional formulas defining sufficient conditions and consistency constraints for each diagnosis (e.g., $d \Rightarrow \neg d'$). To construct \mathcal{K} , we employ a large language model (GPT-5.2) to autoformalize established clinical guidelines into candidate propositional rules, which are subsequently audited and refined by a team of clinicians to guarantee ontological correctness and exhaustiveness.

Because deterministic verification over natural language is intractable, we introduce an autoformalization function \mathcal{T} that maps R_F to a structured evidence assignment. We implement \mathcal{T} for evaluation purposes under a closed-world assumption (CWA), mirroring the clinical reporting standard where significant findings not mentioned are implicitly deemed absent. \mathcal{T} yields a binary state vector $V \in \{1, 0\}^{|\mathcal{F}|}$, where for each $f_i \in \mathcal{F}$:

$$V_i = \begin{cases} 1 & \text{if } f_i \text{ is explicitly affirmed in } R_F, \\ 0 & \text{otherwise (explicitly negated, unmentioned, or underspecified).} \end{cases}$$

We implement \mathcal{T} via a strictly constrained LLM (GPT-OSS-20B, temperature 0.0) enforcing a schema-aligned JSON output to ensure deterministic structural parsing. We analogously extract the asserted diagnoses $D(R_I) \subseteq \mathcal{D}$ from the *Impression* section via strict schema-constrained string matching.

2.2 Diagnostic Entailment via Satisfiability

We frame report verification as a formal satisfiability (SAT) problem. Let Φ_V denote the propositional context induced by the autoformalized findings vector V , constructed as a conjunction of all asserted literals:

$$\Phi_V \equiv \bigwedge_{\{i|V_i=1\}} f_i \wedge \bigwedge_{\{i|V_i=0\}} \neg f_i$$

For any claimed diagnosis $d \in D(R_I)$, we test if d is a logical consequence of the evidence under the knowledge base ($\Phi_V \wedge \mathcal{K} \models d$). We compile \mathcal{K} into SMT constraints and use the Z3 solver as a deterministic decision procedure to check the satisfiability of the negated conclusion:

$$\text{ISAT}(\Phi_V \wedge \mathcal{K} \wedge \neg d)$$

Because the SMT solver is sound and complete, this formulation provides a mathematical proof of entailment, directly inducing a reference-free, runtime-deployable taxonomy of reasoning errors strictly based on internal consistency:

1. **Supported (Entailed):** $d \in D(R_I)$ and the check is UNSAT. Every valid model of the stated Findings forces the diagnosis d .
2. **Unsupported (Hallucinated):** $d \in D(R_I)$ but the check is SAT. The diagnosis is asserted, but there exists a valid state where the Findings hold and d does not.
3. **Missed (Omitted):** $d \in \mathcal{D} \setminus D(R_I)$ and the check is UNSAT. The diagnosis is logically forced by the evidence but absent from the Impression.
4. **Correctly Excluded:** $d \in \mathcal{D} \setminus D(R_I)$ and the check is SAT. The diagnosis is neither forced by the evidence nor claimed.

Verifier Reliability. Deductive guarantees follow a formal assume-guarantee paradigm, conditioned on the VLM’s visual grounding of R_F and the translational fidelity of \mathcal{T} . In this assistive workflow, the radiologist validates perceptual assertions, while autoformalization uncertainty is quantified and surfaced via grammar entropy [8] during clinical review.

3 Experiments and Analysis

3.1 Datasets and VLMs

We evaluate whether neurosymbolic verification can accurately characterize reasoning quality and improve diagnostic performance in radiology reports.

Models. Our experiments span multiple model families and medical adaptation regimes, benchmarking three general-purpose VLMs (Qwen3-VL-8B, Llava-Mistral-7B, Llava-Vicuna-7B) and four domain-adapted medical VLMs (Med Gemma-4B, MedGemma-27B, Lingshu-7B, Lingshu-32B).

Datasets. We test on standard chest radiograph corpora divided into two evaluation regimes. First we look at paired-report datasets, but without ground truth classification diagnosis. specifically MIMIC-CXR [14], Indiana-IU, and CheXpert-Plus [6]. These are used to compute baseline lexical overlap against ground-truth human reports. Next, we look at datasets with ground truth classification labels, CheXpert [12], NIH-CXR[25] to quantify diagnostic performance using structured ground-truth labels. For each image, models are prompted to generate a report containing distinct *Findings* (R_F) and *Impression* (R_I) sections. We apply the autoformalizer \mathcal{T} to extract a structured findings assignment V and an impression diagnosis set $D(R_I)$. All verification is performed using the Z3 solver with the fixed clinical knowledge base \mathcal{K} .

3.2 Baseline: Lexical Overlap

We first evaluate report quality using standard n -gram overlap metrics (BLEU and ROUGE-L) on the paired-report datasets. As shown in Table 1, overlap scores are near-zero across all model families and scales. Clinically equivalent phrasing (e.g., “blunted costophrenic angle” vs. “trace pleural effusion”) is heavily penalized by these metrics. The severe drop between Findings ROUGE-L and Impression ROUGE-L further illustrates that lexical similarity is an inadequate proxy for evaluating deductive clinical reasoning.

Model	Findings		Impression		Full Report	
	BLEU	ROUGE-L	BLEU	ROUGE-L	BLEU	ROUGE-L
Lingshu-7B	0.0235	0.1875	0.0114	0.0787	0.0205	0.1719
Lingshu-32B	0.0237	0.1809	0.0155	0.0860	0.0196	0.1667
Llava-Mistral-7B	0.0040	0.0703	0.0029	0.0229	0.0039	0.0689
Llava-Vicuna-7B	0.0051	0.0834	0.0028	0.0368	0.0046	0.0794
MedGemma-4B	0.0138	0.1295	0.0081	0.0731	0.0127	0.1236
MedGemma-27B	0.0110	0.1266	0.0034	0.0379	0.0108	0.1258
Qwen3-VL-8B	0.0032	0.0670	0.0018	0.0256	0.0020	0.0437

Table 1: BLEU and ROUGE-L overlap between generated and ground-truth reports across Findings, Impression, and Full Report sections, showing that lexical metrics poorly reflect clinical reasoning quality.

3.3 Reference-Free Auditing of Internal Consistency

To evaluate internal logic without relying on external ground truth, we apply our neurosymbolic verifier to test entailment between the generated evidence (Φ_V) and the claimed diagnoses ($D(R_I)$). We formally define two novel reference-free metrics to quantify a model’s deductive reliability. The knowledge base for each dataset was curated separately and audited by a clinician; it covers the diagnosis labels required by that dataset and includes the major diagnostic rules/conditions based on expert opinion.

Let E_V represent the set of all diagnoses logically entailed by the observed findings under the knowledge base, defined as $E_V = \{d \in \mathcal{D} \mid \Phi_V \wedge \mathcal{K} \models d\}$. We define **Soundness** (S) as the proportion of generated impression claims that are logically supported by the findings, and **Completeness** (C) as the proportion of logically entailed diagnoses that the model successfully verbalizes:

$$S = \frac{|E_V \cap D(R_I)|}{|D(R_I)|}; C = \frac{|E_V \cap D(R_I)|}{|E_V|}$$

Inspired by the concept of soundness in formal logic, we target $S \geq \mathbf{0.99}$ [1] for safety-critical clinical deployments, ensuring that incorrect or unsupported validity claims are exceedingly rare.

Model	N	Precision	Recall	F1	Soundness	Completeness	Specificity
Lingshu-7B	4056	0.5340	0.3588	0.4292	0.9562	0.9103	0.9491
Lingshu-32B	4062	0.6183	0.4293	0.5068	0.9636	0.9217	0.9579
Llava-Mistral-7B	4059	0.5323	0.2409	0.3317	0.9702	0.8930	0.9653
Llava-Vicuna-7B	4061	0.4749	0.1997	0.2812	0.9555	0.8387	0.9442
MedGemma-4B	4050	0.6759	0.5432	0.6023	0.9652	0.9389	0.9598
MedGemma-27B	4062	0.7850	0.7113	0.7463	0.9811	0.9721	0.9791
Qwen3-VL-8B	3787	0.9436	0.4279	0.5888	0.9943	0.8735	0.9927

Table 2: Reference-free evaluation (aggregated as mean across datasets) of deductive reliability using neurosymbolic entailment. Precision, recall, F1, soundness, completeness, and specificity quantify how well Impression diagnoses are logically supported by generated Findings.

Applying this logical audit exposes three distinct VLM failure modes that remain invisible to standard lexical metrics. We first observe clinically consistent models (e.g., MedGemma-27B). These models exhibit balanced, high soundness and completeness. Claims are reliably supported by findings, and logically forced conclusions are consistently verbalized in the impression. Next, there are conservative observer models (e.g., Qwen3-VL-8B). These models optimize for soundness at the expense of completeness. The model rarely hallucinates an unsupported diagnosis, but frequently fails to deduce and report diagnoses that are mathematically forced by its own observed findings. Finally, the highest amount of stochasticity comes in models like Llava-Vicuna-7B. They are characterized

by low precision and low completeness, these models treat the reporting task as statistical text generation rather than grounded reasoning, frequently hallucinating impression statements entirely unsupported by prior evidence. We additionally performed manual spot-checking of 100 text-to-SMT translations by formal verification experts and found no translation errors in this sampled set. As is standard in formal verification, our guarantees are conditional (precondition/postcondition style): correctness holds relative to the assumed correctness of the text-to-symbolic translation and the curated knowledge base, rather than as an unconditional clinical guarantee.

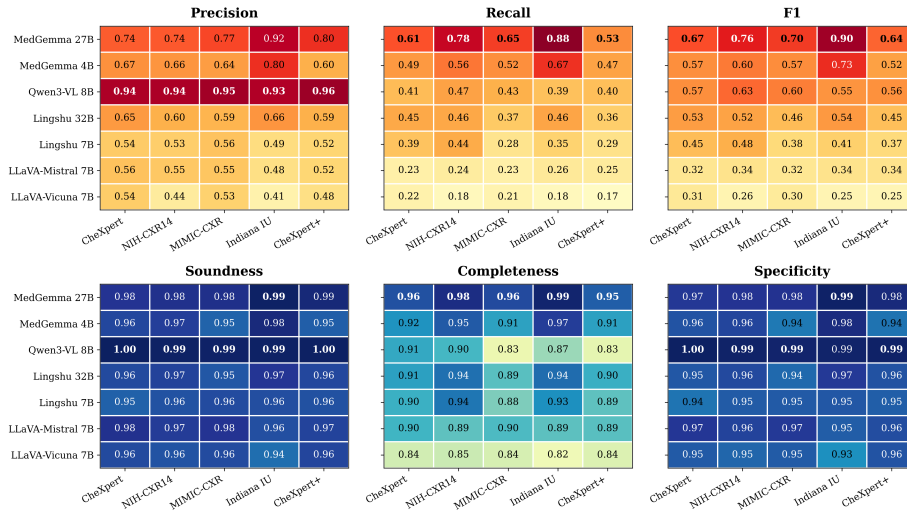


Fig. 2: Heatmap of model performance under neurosymbolic auditing across precision, recall, F1, soundness, completeness, and specificity, revealing distinct reasoning profiles across VLM families.

3.4 Impact of Symbolic Filtering (on Labeled Datasets)

We evaluate the effect of solver-based verification on datasets with structured ground-truth labels by comparing diagnoses extracted from the raw VLM impression (VLM) with the subset of diagnoses that remain after symbolic entailment filtering (OURS). We define the verification delta as $\Delta = \text{OURS} - \text{VLM}$.

Table 3 shows a consistent pattern across both CheXpert and NIH-CXR14: enforcing entailment increases *soundness* for every model, while slightly reducing *completeness*. This behavior is expected because OURS only retains diagnoses that are *deductively licensed* by the evidence extracted from the Findings section under \mathcal{K} . As a result, some diagnoses that were previously stated in the impression, or that match ground-truth labels, may be removed if the necessary supporting evidence is not present (or not extracted) in R_F . Importantly, the decrease in completeness is uniformly small across models and datasets, indicating that verification does not broadly suppress diagnoses that are logically

entailed; rather, it preserves the majority of entailed conclusions while improving consistency. Across all models, Δ Precision is uniformly positive and Δ Recall uniformly negative, indicating that symbolic verification acts as a conservative post-hoc filter that removes impression claims unsupported by the model’s stated evidence, improving precision, internal consistency, and auditability at a small cost in sensitivity (recall).

Model	Soundness			Completeness			Other Deltas	
	VLM	Ours	Δ	VLM	Ours	Δ	Δ Recall	Δ Prec.
CheXpert								
MedGemma-27B	0.9301	0.9599	0.0298	0.8231	0.8107	-0.0124	-0.0601	0.0024
MedGemma-4B	0.9115	0.9311	0.0196	0.8589	0.8465	-0.0124	-0.0600	0.0098
Llava-Mistral-7B	0.9246	0.9684	+0.0438	0.8140	0.8062	-0.0078	-0.0379	+0.0736
Llava-Vicuna-7B	0.9061	0.9458	0.0397	0.8212	0.8126	-0.0086	-0.0416	0.0327
Lingshu-7B	0.9182	0.9494	0.0312	0.8436	0.8246	-0.0190	-0.0918	0.0034
Lingshu-32B	0.9125	0.9426	0.0301	0.8379	0.8248	-0.0131	-0.0637	0.0161
Qwen3-VL-8B	0.9631	0.9689	0.0058	0.8151	0.8128	-0.0023	-0.0111	0.0132
NIH-CXR14								
MedGemma-27B	0.9505	0.9780	0.0275	0.9488	0.9460	-0.0028	-0.0334	+0.1784
MedGemma-4B	0.9090	0.9343	0.0253	0.9462	0.9432	-0.0030	-0.0358	0.0433
Llava-Mistral-7B	0.9223	0.9659	+0.0436	0.9318	0.9269	-0.0049	-0.0589	0.0708
Llava-Vicuna-7B	0.8997	0.9385	0.0388	0.9335	0.9269	-0.0066	-0.0779	0.0018
Lingshu-7B	0.9231	0.9585	0.0354	0.9403	0.9360	-0.0043	-0.0509	0.0844
Lingshu-32B	0.9365	0.9665	0.0300	0.9395	0.9359	-0.0036	-0.0437	0.1015
Qwen3-VL-8B	0.9582	0.9713	0.0131	0.9271	0.9263	-0.0008	-0.0104	0.0522

Table 3: Comparison of raw VLM impressions and our verified diagnoses on labeled datasets. Enforcing entailment increases soundness and precision while reducing completeness and recall.

4 Conclusion

We present a neurosymbolic verification framework for radiology VLM reports that audits whether Impression diagnoses are logically supported by the model’s own Findings using autoformalization, a clinician-audited knowledge base, and SMT solving. Our results show that this enables reference-free measurement of deductive reliability, exposes clinically important reasoning errors missed by lexical metrics, and provides a practical post-hoc safeguard that consistently improves soundness and precision on labeled datasets with only modest recall and completeness trade-offs. More broadly, this shifts evaluation from surface text similarity toward verifiable internal consistency, offering a concrete path to safer and more auditable generative clinical assistants under explicit assume-guarantee conditions common in the domain of formal verification.

Bibliography

- [1] Bayless, S., Buliani, S., Cassel, D., Cook, B., Clough, D., Delmas, R., Dillo, N., Erata, F., Feng, N., Giannakopoulou, D., et al.: A neurosymbolic approach to natural language formalization and verification. arXiv preprint arXiv:2511.09008 (2025)
- [2] Bender, E.M., Gebru, T., McMillan-Major, A., Shmitchell, S.: On the dangers of stochastic parrots: Can language models be too big? In: Proceedings of the 2021 ACM conference on fairness, accountability, and transparency. pp. 610–623 (2021)
- [3] Biere, A., Järvisalo, M., Kiesl, B.: Preprocessing in sat solving. *Handbook of Satisfiability* **336**(2021), 391–435 (2021)
- [4] Brady, A.P., Neri, E.: Artificial intelligence in radiology—ethical considerations. *Diagnostics* **10**(4), 231 (2020)
- [5] Brown, T., Mann, B., Ryder, N., Subbiah, M., Kaplan, J.D., Dhariwal, P., Neelakantan, A., Shyam, P., Sastry, G., Askell, A., et al.: Language models are few-shot learners. *Advances in neural information processing systems* **33**, 1877–1901 (2020)
- [6] Chambon, P., Delbrouck, J.B., Sounack, T., Huang, S.C., Chen, Z., Varma, M., Truong, S.Q., Chuong, C.T., Langlotz, C.P.: Chexpert plus: Augmenting a large chest x-ray dataset with text radiology reports, patient demographics and additional image formats. arXiv preprint arXiv:2405.19538 (2024)
- [7] Ganguly, D., Iyengar, S., Chaudhary, V., Kalyanaraman, S.: PROOF OF THOUGHT : Neurosymbolic program synthesis allows robust and interpretable reasoning. In: The First Workshop on System-2 Reasoning at Scale, NeurIPS’24 (2024), <https://openreview.net/forum?id=Pxx3r14j3U>
- [8] Ganguly, D., Singh, V., Sankar, S., Zhang, B., Zhang, X., Iyengar, S., Han, X., Sharma, A., Kalyanaraman, S., Chaudhary, V.: Grammars of formal uncertainty: When to trust LLMs in automated reasoning tasks. In: The Thirty-ninth Annual Conference on Neural Information Processing Systems (2025), <https://openreview.net/forum?id=QfKpJ00t2L>
- [9] Goddard, K., Roudsari, A., Wyatt, J.C.: Automation bias: a systematic review of frequency, effect mediators, and mitigators. *Journal of the American Medical Informatics Association* **19**(1), 121–127 (2012)
- [10] Hamilton, K., Nayak, A., Božić, B., Longo, L.: Is neuro-symbolic ai meeting its promises in natural language processing? a structured review. *Semantic Web* **15**(4), 1265–1306 (2024)
- [11] Hitzler, P., Sarker, M., Besold, T., Garcez, A., Bader, S., Bowman, H., Domingos, P., Hitzler, P., Kühnberger, K., Lamb, L., et al.: Neural-symbolic learning and reasoning: A survey and interpretation. *Frontiers in artificial intelligence and applications* **342**, 1–51 (2022)
- [12] Irvin, J., Rajpurkar, P., Ko, M., Yu, Y., Ciurea-Ilcus, S., Chute, C., Marklund, H., Haghgoo, B., Ball, R., Shpanskaya, K., et al.: Chexpert: A large chest radiograph dataset with uncertainty labels and expert comparison. In:

- Proceedings of the AAAI conference on artificial intelligence. vol. 33, pp. 590–597 (2019)
- [13] Ji, Z., Lee, N., Frieske, R., Yu, T., Su, D., Xu, Y., Ishii, E., Bang, Y.J., Madotto, A., Fung, P.: Survey of hallucination in natural language generation. *ACM computing surveys* **55**(12), 1–38 (2023)
 - [14] Johnson, A.E., Pollard, T.J., Berkowitz, S.J., Greenbaum, N.R., Lungren, M.P., Deng, C.y., Mark, R.G., Horng, S.: Mimic-cxr, a de-identified publicly available database of chest radiographs with free-text reports. *Scientific data* **6**(1), 317 (2019)
 - [15] Lin, C.Y.: Rouge: A package for automatic evaluation of summaries. In: *Text summarization branches out*. pp. 74–81 (2004)
 - [16] Marcus, G., Davis, E.: *Rebooting AI: Building artificial intelligence we can trust*. Vintage (2019)
 - [17] Moor, M., Banerjee, O., Abad, Z.S.H., Krumholz, H.M., Leskovec, J., Topol, E.J., Rajpurkar, P.: Foundation models for generalist medical artificial intelligence. *Nature* **616**(7956), 259–265 (2023)
 - [18] Papineni, K., Roukos, S., Ward, T., Zhu, W.J.: Bleu: a method for automatic evaluation of machine translation. In: *Proceedings of the 40th annual meeting of the Association for Computational Linguistics*. pp. 311–318 (2002)
 - [19] Parasuraman, R., Manzey, D.H.: Complacency and bias in human use of automation: An attentional integration. *Human factors* **52**(3), 381–410 (2010)
 - [20] Radford, A., Kim, J.W., Hallacy, C., Ramesh, A., Goh, G., Agarwal, S., Sastry, G., Askell, A., Mishkin, P., Clark, J., et al.: Learning transferable visual models from natural language supervision. In: *International conference on machine learning*. pp. 8748–8763. PmLR (2021)
 - [21] Singh, V., Cassel, D., Weir, N., Feng, N., Bayless, S.: Verge: Formal refinement and guidance engine for verifiable llm reasoning. *arXiv preprint arXiv:2601.20055* (2026)
 - [22] Smit, A., Jain, S., Rajpurkar, P., Pareek, A., Ng, A.Y., Lungren, M.: Combining automatic labelers and expert annotations for accurate radiology report labeling using bert. In: *Proceedings of the 2020 conference on empirical methods in natural language processing (EMNLP)*. pp. 1500–1519 (2020)
 - [23] Tu, T., Azizi, S., Driess, D., Schaekermann, M., Amin, M., Chang, P.C., Carroll, A., Lau, C., Tanno, R., Ktena, I., et al.: Towards generalist biomedical ai. *Nejm Ai* **1**(3), AIoa2300138 (2024)
 - [24] Valmееkam, K., Olmo, A., Sreedharan, S., Kambhampati, S.: Large language models still can’t plan (a benchmark for llms on planning and reasoning about change). In: *NeurIPS 2022 Foundation Models for Decision Making Workshop* (2022)
 - [25] Wang, X., Peng, Y., Lu, L., Lu, Z., Bagheri, M., Summers, R.M.: Chestx-ray8: Hospital-scale chest x-ray database and benchmarks on weakly-supervised classification and localization of common thorax diseases. In: *2017 IEEE Conference on Computer Vision and Pattern Recognition (CVPR)*. pp. 3462–3471 (2017). <https://doi.org/10.1109/CVPR.2017.369>